PHYSICAL REVIEW LETTERS

VOLUME 26 | 14 JUNE 1971 | NUMBER 24

Eigenstates of Optical Potentials for Exotic Atoms

Justus H. Koch,* Morton M. Sternheim,* and James F. Walker
Department of Physics and Astronomy, University of Massachusetts, Amherst, Massachusetts 01002
(Received 25 March 1971)

Variations of exotic-atom energy levels and widths with the strength of the nuclear interaction are explained with the aid of a soluble model.

In a recent Letter,[1] Krell has shown that the calculated energy levels and widths for exotic atoms (e.g., K-mesonic atoms) vary in a quite unexpected fashion with the strength of the assumed nuclear interaction. With the aid of a suitable solvable model, we have obtained a simple explanation for these results.

Krell solved the Klein-Gordon equation numerically for point Coulomb potential plus an optical potential of the form $V \propto (\mathrm{Re}A_0 + i\,\mathrm{Im}A_0)\rho$, where A_0 is the K-nucleon scattering length and ρ is the nuclear density. He found two effects: (1) For large values of $\mathrm{Im}A_0$, the optical potential was *repulsive*, i.e., it decreased the binding energy from the point Coulomb value, even in the presence of an attractive real potential. (2) For intermediate values of $\mathrm{Im}A_0$, the calculated energies and widths each exhibited *oscillations* (about 90° out of phase with one another) as $\mathrm{Re}A_0$ was increased. The oscillations were similar in appearance to those obtained with our model and shown in Fig. 1.

Despite the relatively small energy shifts produced by the K-nucleus interaction, perturbation

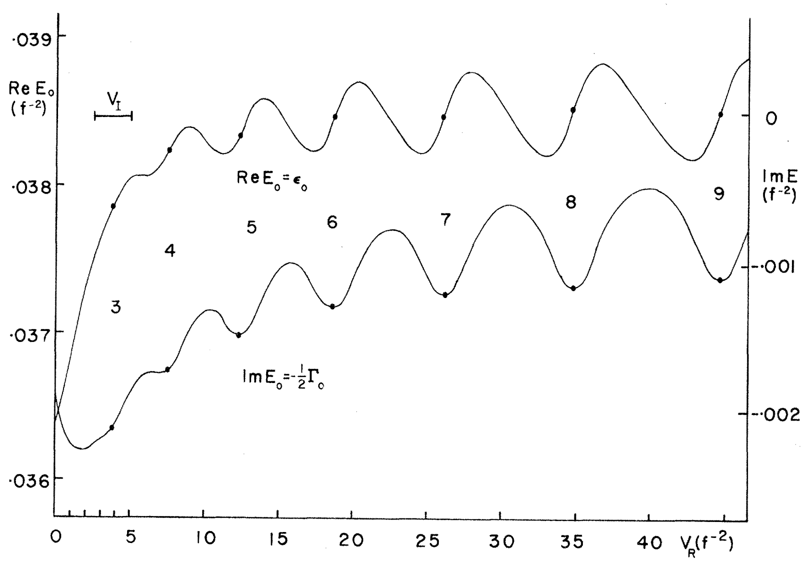

FIG. 1. Energy E_0 of the lowest outer state as a function of V_R for $V_I = 2.5\ \mathrm{F}^{-2}$. The closed circles mark the V_R values at which an inner state ($n_i \geq 3$) "crosses" E_0 as determined using Eq. (4).

theory cannot be used to understand these effects. First-order perturbation theory gives only a crude estimate of the exact shifts. In second order, large contributions arise from intermediate states high in the continuum. It is only the smallness of the atomic wave functions of interest inside nuclear dimensions which makes the expectation value of the very strong nuclear potential so small. Furthermore, Krell's results clearly rule out eigenvalues which are rapidly converging power series in the strength of the optical potential.

For a strongly absorptive optical potential, the wave function goes to zero rapidly inside the nucleus. Thus the meson never "sees" the strong Coulomb attraction at short distances, tending to reduce the binding. Turning on an attractive real optical potential can have only relatively minor effects, since the wave function barely penetrates the nucleus. These minor effects, however, can produce oscillations. We will see this below in our solvable model after some preliminary considerations.

First let us study the Schrödinger equation for an imaginary potential "barrier,"

$$V=0, \quad x>0,$$
$$V=-iV_I, \quad x<0.$$

Let the wave number for $x>0$ be k; the energy is $E=k^2$. (We use $2m=\hbar=1$.) The wave number K for $x<0$ satisfies $K^2=E-V=k^2+iV_I$. If k is real (or almost real) and $|k|^2 \lesssim V_I$, then K has a large imaginary part. Thus for $x<0$ the wave will in general be a sum of increasing and decreasing terms. One can, however, find standing waves for $x>0$ which fit smoothly onto exponentially decreasing terms for $x<0$.

Similarly, if K is nearly real and $|K|^2 \leq V_I$, then we find generally an exponential superposition for $x>0$. Again, standing waves exist for $x<0$, fitting smoothly onto decreasing terms for $x>0$.

We see, therefore, that the barrier acts identically for waves with real wave numbers on either side of $x=0$. It causes them to have exponential behavior on the opposite side.

Second, we note that for complex κ, a standing wave $\sin\kappa x$ has no zeros (except at $x=0$). However, with $\kappa=\kappa_R+i\kappa_I$,

$$|\sin\kappa x|^2=\sin^2\kappa_R x+\sinh^2\kappa_I x$$

is a sum of oscillating and exponentially increasing positive terms, and has "dips" when $\kappa_R x=n\pi$. The number of dips apparently characterizes the eigenstates of complex potentials in the same way as does the number of nodes for real potentials.

Our solvable model is a nonrelaticistic s-wave particle in a spherical box of radius r_A containing a complex square well of depth $V=-V_R-iV_I$ and radius r_N. In numerical examples, we use $r_A=20$ F and $r_N=4$ F to simulate the respective atomic and nuclear radii. A state with energy $E=\epsilon-i\frac{1}{2}\Gamma$ has wave numbers given by

$$K^2=E-V, \quad r<r_N;$$
$$k^2=E, \quad r_N<r<r_A. \tag{1}$$

Its wave function is proportional to $r^{-1}\sin Kr$ for $r<r_N$, and to $r^{-1}\sin k(r_A-r)$ for $r_N<r<r_A$. Its energy satisfies

$$K\cot Kr_N=-k\cot k(r_A-r_N). \tag{2}$$

The roots of (2) are obtained by searching in two dimensions starting from the familiar $V=0$ eigenvalues, $E=(n\pi/r_A)^2$, $n=1, 2, 3, \cdots$.

For the case of strong absorption and no attraction, $V=-iV_I$, two distinct types of eigenstates exist: "inner states" and "outer states." This has already been suggested by our discussion of the imaginary barrier. For an inner state, the wave number in the inner region ($r<r_N$) is nearly real. The wave function is strongly attenuated outside of r_N, and $\Gamma \approx 2V_I$. For an outer state, the wave number in the outer region ($r_N<r<r_A$) is nearly real. The wave function is strongly attenuated in the inner region, and $\Gamma \ll 2V_I$ [see Fig. 2(a)]. In the limit of very large V_I, this separation becomes complete, and the energies approach the appropriate spherical-box values:

$$E_i=(n_i\pi/r_N)^2-iV_I,$$
$$n_i=1, 2, \cdots \text{ (inner states)};$$
$$E_0=[n_0\pi/(r_A-r_N)]^2,$$
$$n_0=1, 2, \cdots \text{ (outer states)}.$$

In our terminology, the atomic states considered by Krell are outer states.

We now consider the evolution of the spectrum from the $V=0$ limit. First let us increase V_I from zero. Some of the original spherical-box states develop into outer states while others become inner states. For our numerical example, the $n=3$ and 9 states become the two lowest inner states, and the remainder of the first ten states become outer states. Confining the ground state

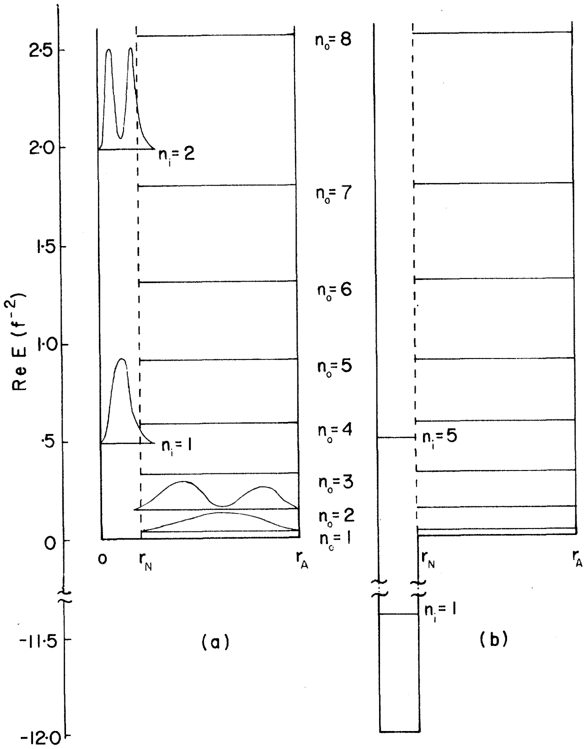

FIG. 2. (a) Level diagram for $V_R=0$ and $V_I=2.5$ F^{-2}. The absorptive region is $r<r_N$. $|\Psi|^2$ is sketched for several levels to show the separation into inner and outer states. (b) Level diagram for $V_R=12$ F^{-2} and $V_I=2.5$ F^{-2}. The $n_i \leq 4$ states are in the nuclear well.

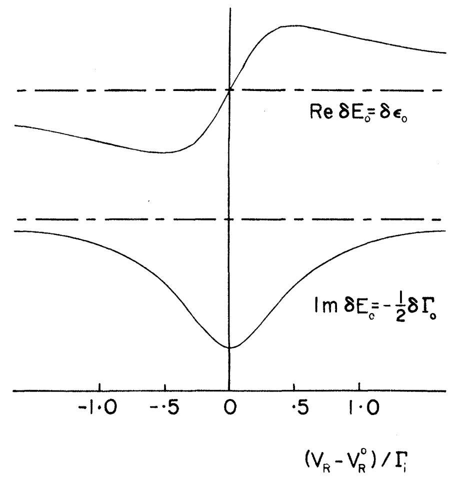

FIG. 3. Dependence of E_0 on V_R due to the energy denominator (3). Since $\delta\epsilon_i \approx -V_R$, the resonant behavior has a width $\Gamma_i \approx 2V_I$. V_R is given relative to V_R^0, the attraction for which $\epsilon_i = \epsilon_0$, in units of Γ_i.

to a smaller region has the effect of raising its energy. This effective repulsion has been stressed by Krell.

Next let us increase the attraction V_R. The inner states are drawn down into the attractive well as shown in Fig. 2(b). The outer states are only slightly affected because of their small penetration into the inner region. However, ϵ_0 and Γ_0 for the lowest outer state Ψ_0 do display oscillations with an amplitude $<10^{-4}V_R$ (see Fig. 1). They do not appear until $V_R/V_I \gtrsim 3$, and their "period" increases with V_R. This period corresponds to the change in V_R needed to add half a wavelength to the inner portion of Ψ_0. Such a change would also add half a wavelength to an inner state Ψ_i if $\epsilon_i = \epsilon_0$. This suggests that the oscillations may be attributed to inner states "crossing" the lowest outer state as they drop into the attractive well.

To verify this conjecture, let us study the coupling between states Ψ_i and Ψ_0 as V_R is increased from zero. Solving the two-level problem gives an inner-state energy shift $\delta E_i \approx -V_R$ because Ψ_i is almost entirely localized in the inner region. We also find a contribution to δE_0 proportional to $V_R^2/(E_0-E_i)$, where the energies are the actual eigenvalues, not the $V_R=0$ limits.[2] Since $\Gamma_0 \ll \Gamma_i$,

$$\frac{1}{E_0-E_i} = \frac{(\epsilon_0-\epsilon_i)-i\frac{1}{2}\Gamma_i}{(\epsilon_0-\epsilon_i)^2+\frac{1}{4}\Gamma_i^2}. \tag{3}$$

This is plotted in Fig. 3. Both real and imaginary parts look roughly like pieces of a sine wave. The former is increasing linearly with V_R (decreasing with ϵ_i) at $\epsilon_i = \epsilon_0$, and the latter has a minimum there. Generalizing now to several inner states coupling to Ψ_0, we expect to observe oscillations in E_0 provided that successive states are separated in energy by more than $\Gamma_i \approx 2V_I$.[3] The values of V_R for which $\epsilon_i = \epsilon_0$ are given by a very simple formula for $V_R \gg V_I$. Since $\epsilon_0 \ll \frac{1}{2}\Gamma_i \approx V_I$, Eqs. (1) become $K^2 \approx V_R$ and $k^2 \approx -iV_I$. Equation (2) then reduces to

$$\cot(V_R^{1/2}r_N) = i(-iV_I/V_R)^{1/2} \approx 0,$$

or

$$V_R^{1/2}r_N = (n_i - \tfrac{1}{2})\pi. \tag{4}$$

Equation (4) gives the values of V_R for which $\epsilon_i = \epsilon_0$; these are shown for $n_i \geq 3$ as solid circles in Fig. 1. The role of the inner states in producing the oscillations is therefore confirmed.

We see then with this example that the repulsion and oscillations found by Krell have a simple explanation. The implications for the phenomenology of exotic atoms have already been noted.[1]

We should expect to observe these effects whenever the absorptive optical potential is strong enough to produce a division into inner and outer states.

To the best of our knowledge, the existence of inner states has not previously been discussed. Of course, any exact solution of the wave equation for the usual problems automatically takes them into account. We hope to study further their physical significance and implications for other experiments.

We wish to thank Professor Max Krell for stimulating discussions and for sending us a preprint of his work. We also thank Professor Robin Tucker for the use of his search program. The computations were performed at the University of Massachusetts Research Computing Center with the aid of a grant from the University.

---

*Research supported in part by the National Science Foundation.

[1]M. Krell, Phys. Rev. Lett. 26, 584 (1971).

[2]These results are obtained by an expansion in powers of the penetration of Ψ_0 into the inner region. They are not an expansion of powers of V_R. Since the Hamiltonian is not Hermitian, its eigenstates are not necessarily orthogonal; this complication does not affect our qualitative discussion.

[3]This can be derived using projection-operator techniques. See H. Feshbach, Ann. Phys. (New York) 5, 537 (1958), and 19, 287 (1962).

Temperature Dependence of Critical Opalescence in Carbon Dioxide*

John A. White and Bruce S. Maccabee
American University, Washington, D. C. 20016
(Received 29 March 1971)

Rayleigh scattering has been studied along the critical isochore and the coexistence curve of carbon dioxide. Measured intensities interpreted according to the theory of Ornstein and Zernike agree with expectation based on classical PVT measurements. It is suggested that over many decades of temperature distance from T_c the PVT and optical data are consistent with a reduced compressibility $(\partial\rho/\partial\mu)_T = \Gamma t^{-\gamma}$, and $\Gamma'(-t)^{-\gamma'}$, with $t=(T-T_c)/T_c$, where $\gamma = 1.17\pm0.02 = \gamma'$ and $\Gamma = 0.072\pm0.006 = 4.1\Gamma'_{\rm gas} \simeq 3.6\Gamma'_{\rm liq}$.

Data have been obtained on the intensity of critical opalescence in carbon dioxide in the supercritical phase along the critical isochore for $T > T_c$ and in the gas and liquid phases close to the coexistence line for $T < T_c$. Intensities were measured for light of wavelength 0.633 μm, scattering angles of 13.5 and 22.5°, and temperatures in the range $10^{-3} \leq |T-T_c| \leq 10$°C.

Measurements were made on CO_2 contained in a scattering cell constructed of stainless steel, with indium and lead seals. It had plane, parallel sapphire windows 5 mm apart which were antireflection coated and oriented so as not to depolarize light. No depolarization was observed with this cell upon filling it to nearly the critical pressure of CO_2. The volume of the cell was adjusted so that at T_c the meniscus appeared at the center. The position of the cell (its height) could be adjusted relative to the incident beam of light to obtain scattering from above, below, or at the meniscus. A narrow beam of light (~0.1 mm diam) from a 4-mW He:Ne laser was used to illuminate the gas in the cell. The intensity of the light was attenuated, for measurements close to T_c, using neutral density filters.

Intensities of the incident and scattered light were measured with an RCA 7265 photomultiplier. The photomultiplier was calibrated by an addition method: Two small light bulbs were placed close together relatively far from an aperture in front of the photomultiplier; the intensities of the two bulbs were made equal as measured by the photocurrent, then added to give a reading for double intensity. The intensity was doubled repeatedly this way to calibrate the photomultiplier over eight decades of intensity. The calibration thus obtained agreed with one based on an assumed linearity of photocurrents below 10^{-7} A and with a calibration based on neutral density filters whose densities were checked by precision densitometers.

The temperature of the cell was controlled to $\lesssim 3\times10^{-4}$°C, with thermal gradients $\lesssim 0.1$ mdeg/cm. Temperatures were measured with a platinum resistance thermometer to a reproducibility of $\sim10^{-3}$ deg.

Two fills of CO_2 were used, each of nominal purity better than 99.99%. The critical temperatures were measured to be $T_c = 30.99 \pm 0.01$°C using the platinum resistance thermometer which